1993ApJ...413L..27F

THE ASTROPHYSICAL JOURNAL, 413:L27–L30, 1993 August 10
© 1993. The American Astronomical Society. All rights reserved. Printed in U.S.A.

PULSED HIGH-ENERGY GAMMA RAYS FROM PSR 1055−52

J. M. FIERRO,[1] D. L. BERTSCH,[2] K. T. BRAZIER,[3] J. CHIANG,[1] N. D'AMICO,[4] C. E. FICHTEL,[2] R. C. HARTMAN,[2] S. D. HUNTER,[2] S. JOHNSTON,[5] G. KANBACH,[3] V. M. KASPI,[6] D. A. KNIFFEN,[7] Y. C. LIN,[1] A. G. LYNE,[8] R. N. MANCHESTER,[5,6] J. R. MATTOX,[2,9] H. A. MAYER-HASSELWANDER,[3] P. F. MICHELSON,[1] C. VON MONTIGNY,[3] P. L. NOLAN,[1] E. SCHNEID,[10] AND D. J. THOMPSON[2]

Received 1993 April 8; accepted 1993 May 27

ABSTRACT

The Energetic Gamma Ray Experiment Telescope (EGRET) aboard the *Compton Gamma Ray Observatory* has detected a high-energy γ-ray source at a position coincident with that of the radio pulsar PSR 1055−52. Analysis of the EGRET data at the radio pulsar period of 197 ms has revealed pulsed γ-radiation at energies above 300 MeV, making PSR 1055−52 the fifth detected high-energy γ-ray pulsar. The pulsed radiation from PSR 1055−52 has a very hard photon spectral index of -1.18 ± 0.16 and a high efficiency for converting its rotational energy into γ-rays. No unpulsed emission was observed.

Subject headings: gamma rays: observations — pulsars: individual (PSR 1055−52)

1. INTRODUCTION

The radio pulsar PSR 1055−52 has been of interest since its discovery by Vaughan & Large (1972). The relatively short period of 197.11 ms and moderate period derivative of 5.8×10^{-15} s s^{-1} imply an average surface magnetic field of 1.2×10^{12} G, a characteristic age of 5.3×10^5 yr, and a rotational energy loss rate of 3.0×10^{34} ergs s^{-1}. From the dispersion measure of 30.1 pc cm^{-3} and the mean free electron density, the distance is calculated to be 1.5 kpc (Taylor, Manchester, & Lyne 1993). McCulloch et al. (1976) showed PSR 1055−52 to be in the small class of radio pulsars with a strong interpulse midway between the main pulses, and noted the overall similarity of its radio light curve to that of the Crab pulsar, in that it has a precursor, main pulse, and strong interpulse. For this reason, Manchester et al. (1978) included PSR 1055−52 in a southern hemisphere search for optical pulsations from selected pulsars, with no positive results.

PSR 1055−52 was detected as a soft X-ray source by the *Einstein Observatory* (Cheng & Helfand 1983) and later by *EXOSAT* (Brinkmann & Ögelman 1987), although neither detection revealed modulation at the pulsar rotation frequency. Recently, Ögelman & Finley (1993) have reported the *ROSAT* detection of X-ray pulsation from PSR 1055−52 at the radio pulsar period. Searches for pulsed γ-ray emission from PSR 1055−52 with both *SAS 2* (Thompson et al. 1983) and *COS B* (Buccheri et al. 1983) gave negative results.

In this *Letter*, five EGRET observations of PSR 1055−52 are presented that establish this source as a high-energy γ-ray pulsar. The observations are discussed in § 2. The pulsed γ-ray light curve and energy spectrum are given in § 3. Finally, in § 4 the characteristics of this source are compared with those of the other four known high-energy γ-ray pulsars.

2. OBSERVATIONS

EGRET has components which are commonly used in high-energy γ-ray telescopes: an anticoincidence system to discriminate against charged particles, a spark chamber system with interspersed pair conversion material to determine the trajectories of the secondary electron-positron pair, a triggering telescope that detects the presence of charged particles with the correct direction of motion, and an energy-measuring calorimeter, which for EGRET is a NaI(Tl) crystal. Descriptions and general capabilities of the instrument are given by Hughes et al. (1980), Kanbach et al. (1988, 1989), Nolan et al. (1992), and Thompson et al. (1993). The telescope covers the energy range from approximately 20 MeV to 30 GeV with more than an order of magnitude greater sensitivity than the *SAS 2* or *COS B* instruments, as well as improved resolution in energy, angle, and timing measurements. Because of the very low flux level of high-energy γ-rays, observing periods are typically about 2 weeks.

Table 1 lists the relevant parameters for the five observations in which PSR 1055−52 was in the field of view. The effective area of the telescope was greatly reduced for those observations in which the source was far away from the EGRET instrument axis. Thus the one observation in which PSR 1055−52 was within 10° of the instrument axis has a greater exposure to the source than the other four viewing periods combined. The exposure to the source was calculated from the known telescope sensitivity as a function of operating mode and energy (Thompson et al. 1993) and the known times of occultations, etc. Standard EGRET data processing operations (Bertsch et al. 1989) were performed to provide optimal estimates of the direction and energy of each photon.

[1] W. W. Hansen Experimental Physics Laboratory, Stanford University, Stanford, CA 94305-4085.
[2] NASA/Goddard Space Flight Center, Code 662, Greenbelt, MD 20771.
[3] Max-Planck-Institut für Extraterrestrische Physik, D-8046 Garching, Germany.
[4] Istituto di Fisica dell'Università di Palermo and Istituto di Radioastronomie del CNR, I-40126 Bologna, Italy.
[5] Australia Telescope National Facility, CSIRO, P.O. Box 76, Epping, New South Wales 2121, Australia.
[6] Department of Physics, Princeton University, Princeton, NJ 08544.
[7] Hampden-Sydney College, P.O. Box 862, Hampden-Sydney, VA 23943.
[8] Nuffield Radio Astronomy Laboratories, Jodrell Bank, University of Manchester, Macclesfield, Cheshire SK11 9DL, UK.
[9] Compton Observatory Science Support Center, Astronomy Programs, Computer Sciences Corporation, NASA/GSFC, Code 668.1, Greenbelt, MD 20771.
[10] Grumman Aerospace Corporation, Mail Stop A01-26, Bethpage, L.I., NY 11714.

© American Astronomical Society • Provided by the NASA Astrophysics Data System

1993ApJ...413L..27F

TABLE 1

EGRET PARAMETERS FOR OBSERVATIONS OF PSR 1055−52

OBSERVATION DATES	POINTING DIRECTION l	POINTING DIRECTION b	ASPECT ANGLE	EXPOSURE $E > 100$ MeV (cm^2 s)
1991 May 10–16	266°.32	0°.74	20°.5	5.45×10^7
1991 Aug 22–Sep 5	262.94	−5.67	26.1	1.18×10^8
1991 Oct 17–31	310.71	22.21	28.5	8.68×10^7
1991 Nov 14–28	285.04	−0.74	7.4	366×10^8
1992 Jun 25–Jul 2	284.20	22.89	16.3	5.78×10^7

3. RESULTS

Maximum-likelihood analysis of the spatial distribution of γ-rays (Mattox et al. 1993) revealed a γ-ray point source above 100 MeV at a location $l = 286°.06$, $b = 6°.39$ with a 68% confidence radius of 0°.4. The radio position of PSR 1055−52 lies within this error box. Table 2 lists the results of the γ-ray spatial analysis of the region surrounding PSR 1055−52 for the five observations combined, showing the flux and significance of the γ-ray excess for three different energy ranges. Source fluxes were derived using the detector point-spread function to model any excess detected above the expected diffuse γ-ray background (Bertsch et al. 1993). The maximum-likelihood analysis indicates that the source has a high significance above 100 and 300 MeV, and remains prominent above 1000 MeV.

The only convincing method with which to establish the identity of the γ-ray source as PSR 1055−52 is to find modulation of the γ-ray light curve at the period of the radio pulsation. Radio timing parameters for PSR 1055−52 based on contemporaneous 1520 MHz radio observations made at the Parkes Observatory are listed in Table 3. For all five observations, γ-rays arriving within an energy-dependent cone of half-angle $\theta_{max} = 5°.85 \times (E_\gamma/100\ \mathrm{MeV})^{-0.534}$, with photon energy E_γ in MeV, about the position of PSR 1055−52 were selected (Thompson et al. 1993). In addition, to screen out the Earth albedo γ-rays at a 4 σ confidence level, only those γ-rays arriving within a zenith angle $\phi \leq 110° - 4\theta_{max}$ were used. The arrival times of the selected γ-rays were transformed to solar system barycentric time and epoch folded according to the radio timing parameters.

TABLE 2

TOTAL FLUX FROM PSR 1055−52

Energy Range	Flux (cm^{-2} s^{-1})	Significance
$E > 100$ MeV	$(2.7 \pm 0.5) \times 10^{-7}$	5.8 σ
$E > 300$ MeV	$(1.6 \pm 0.3) \times 10^{-7}$	8.2 σ
$E > 1000$ MeV.....	$(3.0 \pm 1.1) \times 10^{-8}$	4.3 σ

TABLE 3

RADIO TIMING PARAMETERS USED IN GAMMA-RAY PERIODIC ANALYSIS OF PSR 1055−52

Parameter	Value
Right ascension (J2000)	$10^h57^m58^s.910$
Declination (J2000)	−52°26′56″.14
Frequency	5.0733051243399 Hz
Frequency derivative	-1.50111×10^{-13} Hz s^{-1}
Epoch (MJD)	48,626

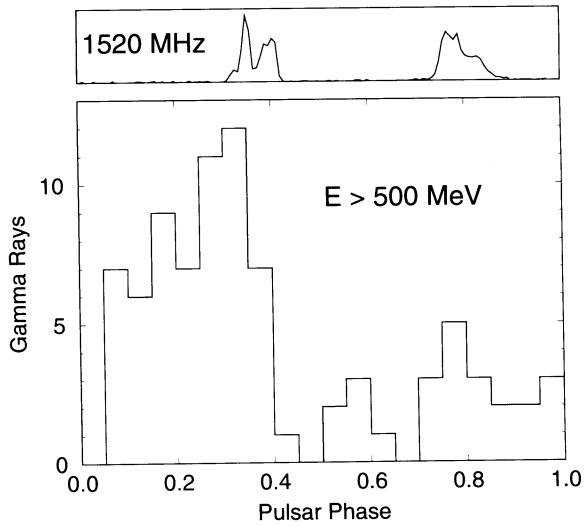

FIG. 1.—Pulse profiles of PSR 1055−52. The top panel shows the radio profile at a frequency of 1520 MHz. The lower panel shows the combined γ-ray data above 500 MeV for the five EGRET observations of the PSR 1055−52 epoch folded using the radio pulsar ephemeris.

Figure 1 shows the resulting γ-ray light curve for energies above 500 MeV. For comparison, the radio pulse profile at 1520 MHz is also shown. A broad γ-ray pulse that spans roughly 35% of the pulse period leads the highest radio peak. Although Figure 1 includes data from all five observations, only 84 photons meet the selection criteria, owing to the limited exposure to the source. The light-curve distribution in Figure 1 has a χ^2 value of 59.8 with 19 degrees of freedom, indicating that the probability that this is drawn from a random distribution is $\sim 4 \times 10^{-6}$. Using the bin-independent H-test (de Jager, Swanepoel, & Raubenheimer 1988), a value of 42.4 is found, corresponding to a random distribution probability of less than 3×10^{-7}. Below 300 MeV, the signal becomes hard to distinguish above the diffuse Galactic radiation.

Following the method used by Nolan et al. (1993) to determine the pulsed energy spectrum, the photons were divided into separate energy intervals, and selected for analysis based on an energy-dependent acceptance cone centered about the source position. From Figure 1, the pulsed phase interval was estimated to span from 0.05 to 0.40 of the phase interval, while the γ-rays outside this range were assumed to be due to background. For each energy interval, the total number of γ-rays falling within the pulsed phase interval was adjusted by subtracting the scaled background to get the estimated number of γ-rays due to source pulsation. Taking into account the EGRET instrumental response functions (Thompson et al. 1993), a model based on a power law was fitted to the data using a least-squares method. Figure 2 shows the derived pulsed spectrum for the combined EGRET observations of PSR 1055−52. The pulsed spectrum is well represented between 100 MeV and 4 GeV by a single power law of the form

$$\frac{dN}{dE_\gamma} = (1.91 \pm 0.25) \times 10^{-10} \left(\frac{E_\gamma}{908\ \mathrm{MeV}}\right)^{-1.18 \pm 0.16}$$

$$\text{photons cm}^{-2}\ \text{s}^{-1}\ \text{MeV}^{-1}\ . \quad (1)$$

The energy-scale factor of 908 MeV has been chosen so that the statistical errors in the power-law index and the overall

© American Astronomical Society • Provided by the NASA Astrophysics Data System

1993ApJ...413L..27F

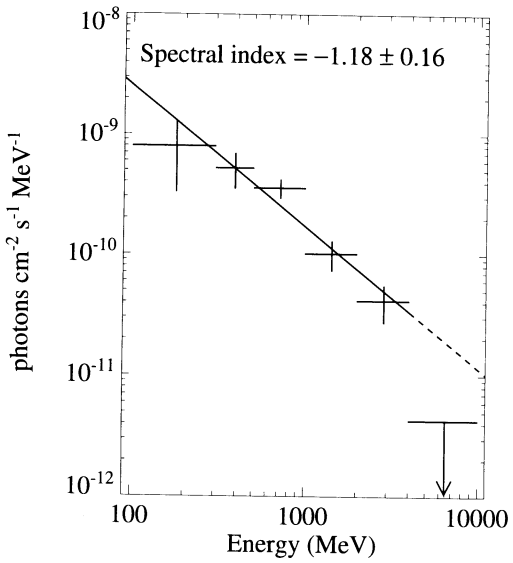

FIG. 2.—Differential photon energy spectrum of PSR 1055−52 during the pulsed phase (0.05–0.40 from Fig. 1).

normalization factor are uncorrelated. The time-averaged spectrum has a normalization factor which is 0.35 that of equation (1). The large uncertainties in equation (1) reflect the limited EGRET exposure to PSR 1055−52. Nevertheless, this spectrum is harder than the pulsed spectrum of any of the other high-energy γ-ray pulsars seen by EGRET. The 2 σ upper limit shown indicates a drop-off in pulsed counts above 4 GeV.

From equation (1) the time-averaged pulsed photon flux between 100 MeV and 4 GeV is determined to be $(2.4 \pm 0.4) \times 10^{-7}$ photons cm^{-2} s^{-1}, which is in good agreement with the total flux above 100 MeV listed in Table 2, suggesting that the γ-ray emission from PSR 1055−52 is due entirely to pulsation. This is evidenced in Figure 1, where there is little or no unpulsed emission apparent.

4. DISCUSSION

It can be argued that those pulsars which have the greatest total energy flux at Earth are the most probable candidates for γ-ray detection. Assuming that the energy emitted from a pulsar is directly proportional to its rotational energy loss $\dot{E}$, the energy flux at Earth is proportional to $\dot{E}/d^2$, where d is the distance to the pulsar. Of the more than 500 known radio pulsars, the high-energy γ-ray pulsars Crab, Vela, and PSR 1706−44 have three of the four highest values of $\dot{E}/d^2$. If the distance to Geminga is taken to be 250 pc (Ruderman et al. 1992), it has a value of $\dot{E}/d^2$ that is 5×10^{-3} of the Crab value, which would place it seventh among all known pulsars. In contrast, PSR 1055−52, with a value which is 10^{-4} the Crab value, has only the 25th highest value of $\dot{E}/d^2$.

The fact that PSR 1055−52 was detected as a γ-ray source despite its relatively small expected energy flux implies that PSR 1055−52 has a high efficiency for converting its rotational energy into high-energy γ-rays. Extrapolating the pulsed spectrum of equation (1) to 5 GeV, the time-averaged energy flux between 100 MeV and 5 GeV is $(4.2 \pm 0.7) \times 10^{-10}$ ergs cm^{-2} s^{-1}. The γ-ray luminosity is defined as $L_\gamma = \Omega F d^2$, where Ω is the beaming solid angle and F is the measured energy flux at a distance d. Using the distance of 1.5 kpc derived from the dispersion measure and assuming beaming into a solid angle of 1 sr, the γ-ray luminosity between 100 MeV and 5 GeV is $(9.4 \pm 1.6) \times 10^{33}$ ergs s^{-1}. This implies that the efficiency for γ-ray production is 31%, which is much higher than that inferred for the other γ-ray pulsars. Table 4 lists the derived characteristics of PSR 1055−52, along with those of the other four known high-energy γ-ray pulsars. For each pulsar, L_γ (100 MeV to 5 GeV) was estimated assuming beaming into a solid angle of 1 sr. The efficiency $\eta = L_\gamma/\dot{E}$ was determined assuming a stellar moment of inertia of 10^{45} g cm^2. Of these pulsars, PSR 1055−52 has the hardest spectral index and highest efficiency. Note that among the high-energy γ-ray pulsars listed in Table 4, the spectrum hardens and the efficiency increases with age. Due to the limited number of sources and the fact that harder sources are more easily detected in the presence of the diffuse background than are softer sources, these trends should be interpreted with caution.

According to the polar cap model (Daugherty & Harding 1982), γ-rays are the result of radiation from the acceleration of primaries in the magnetosphere near the pulsar polar cap surface. Harding (1981) predicts that because of an increase in the current of primary particles, efficiency should increase with apparent age τ and period derivative $\dot{p}$ as $\eta \sim \tau^{1.8}\dot{p}^{1.3}$. An application of this relationship to PSR 1055−52 predicted a possible EGRET detection at about the observed intensity (Thompson 1990). However, most calculations involving the polar cap model assume synchrotron and curvature radiation from a cooling population of electrons, which would have difficulty explaining the observed spectral hardness of PSR 1055−52. In the outer gap model (Cheng, Ho, & Ruderman 1986), primaries are accelerated in vacuum gaps in the outer magnetosphere of the pulsar. The original outer gap model predicted that pulsar efficiency would increase with period until the vacuum gaps become quenched at periods longer

TABLE 4

DERIVED CHARACTERISTICS OF KNOWN HIGH-ENERGY GAMMA-RAY PULSARS

Pulsar	Period (ms)	Age (yr)	Spectral Index	L_γ[a] (ergs s^{-1})	η	References
Crab	33.39	1.3×10^3	-2.15 ± 0.04	4.0×10^{34}	0.00009	1
Vela	89.29	1.1×10^4	-1.89 ± 0.06	2.1×10^{34}	0.0031	2
PSR 1706−44	102.44	1.7×10^4	-1.72 ± 0.08	2.6×10^{34}	0.0076	3
Geminga[b]	237.10	3.4×10^5	-1.46 ± 0.06	2.5×10^{33}	0.076	4, 5
PSR 1055−52	197.11	5.3×10^5	-1.18 ± 0.16	9.4×10^{33}	0.31	

[a] 100 MeV to 5 GeV, beaming into solid angle of 1 sr.
[b] Assumed distance of 250 pc (Ruderman et al. 1992).

REFERENCES.—(1) Nolan et al. 1993; (2) Kanbach et al. 1980; (3) Thompson et al. 1992; (4) Bertsch et al. 1992; (5) Mayer-Hasselwander et al. 1993.

© American Astronomical Society • Provided by the NASA Astrophysics Data System

1993ApJ...413L..27F

than about 130 ms, at which time the pulsars would become incapable of producing γ-rays (Ruderman & Cheng 1988). A modified version of the model contends that pulsar efficiency remains roughly constant until the pulsar approaches a "death line" defined as a function of period and magnetic field (Chen & Ruderman 1993). Near the death line, the efficiency increases steadily until it reaches 100%, after which γ-ray production ceases. PSR 1055−52 falls almost directly on this death line, implying that it is near its peak γ-ray efficiency and is at the very limit of sustaining an outer gap. In addition, the relatively hard spectral index of PSR 1055−52 implies an increased role for the inverse Compton scattering mechanism, which occurs more naturally in the outer gap model.

With the limited EGRET exposure thus far, it is difficult to address issues such as time-variability of the source. Future observations are necessary for a better understanding of the nature of this high-energy γ-ray pulsar. In addition, to examine better the collective properties of these objects, searches for additional high-energy γ-ray pulsars and determinations of upper limits to those not detected (Brazier et al. 1993; Fierro et al. 1993) are important.

The EGRET team gratefully acknowledges support from the following: Bundesministerium für Forschung und Technologie grant 50 QV 9065 (MPE), NASA grant NAG 5-1742 (HSC), NASA grant NAG 5-1605 (SU), and NASA contract NAS 5-31210 (GAC).

REFERENCES

Bertsch, D. L., et al., 1989, in Proc. *Gamma-Ray Observatory* Science Workshop, ed. W. N. Johnson (Greenbelt: NASA), 2-52
Bertsch, D. L., et al. 1992, Nature, 357, 306
Bertsch, D. L., Dame, T. M., Fichtel, C. E., Hunter, S. D., Sreekumar, P., Stacy, J. G., & Thaddeus, P. 1993, ApJ, in press
Brazier, K. T. S., et al. 1993, in preparation
Brinkmann, W., & Ögelman, H. 1987, A&A, 182, 71
Buccheri, R., et al. 1983, A&A, 128, 245
Chen, K., & Ruderman, M. 1993, ApJ, 402, 264
Cheng, A. F., & Helfand, D. J. 1983, ApJ, 271, 271
Cheng, K. S., Ho, C., & Ruderman, M. 1986, ApJ, 300, 500
Daugherty, J. K., & Harding, A. 1982, ApJ, 252, 337
de Jager, O. C., Swanepoel, J. W. H., & Raubenheimer, B. C. 1988, A&A, 221, 180
Fierro, J. M., et al. 1993, in preparation
Harding, A. K. 1981, ApJ, 245, 267
Hughes, E. B., et al. 1980, IEEE Trans. Nucl. Sci., 27, 364
Kanbach, G., et al. 1980, A&A, 90, 163
Kanbach, G., et al. 1988, Space Sci. Rev., 49, 69
Kanbach, G., et al. 1989, in Proc. *Gamma Ray Observatory* Science Workshop, ed. W. N. Johnson (Greenbelt: NASA), 2-1
Manchester, R. N., et al. 1978, MNRAS, 184, 159
Mattox, J. R., et al. 1993, in preparation
Mayer-Hasselwander, H. A., et al. 1993, ApJ, submitted
McCulloch, P. M., Hamilton, P. A., Ables, J. G., & Komesaroff, M. M. 1976, MNRAS, 175, 71P
Nolan, P. L., et al. 1992, IEEE Trans. Nucl. Sci., 39, 993
Nolan, P. L., et al. 1993, ApJ, 409, 697
Ögelman, H., & Finley, J. P. 1993, ApJ, 413, L31
Ruderman, M., Chen, K., Cheng, K. S., & Halpern, J. P. 1992, preprint
Ruderman, M., & Cheng, K. S. 1988, ApJ, 335, 306
Taylor, J. H., Manchester, R. N., & Lyne, A. G. 1993, preprint
Thompson, D. J. 1990, in Proc. EGRET Science Symposium, ed. C. Fichtel (Greenbelt: NASA), 115
Thompson, D. J., Bertsch, D. L., Hartman, R. C., & Hunter, S. D. 1983, A&A, 127, 220
Thompson, D. J., et al. 1992, Nature, 359, 615
Thompson, D. J., et al. 1993, ApJS, 86, 629
Vaughan, A. E., & Large, M. I. 1972, MNRAS, 156, 27P

© American Astronomical Society • Provided by the NASA Astrophysics Data System